Simulation of a wear experiment

J. Andersson[a,], A. Almqvist[a,], R. Larsson[a,]

[a]*Division of Machine Elements,*
Lulea University of Technology, Sweden

Abstract

By using a deterministic FFT-accelerated contact mechanical tool to calculate pressure and elastic-plastic deformation, a wear model is utilized to simulate the time dependent wear from a sphere on flat contact. The results of the simulated wear are compared to experimental results form a SRV ball on disk tribometer, from which worn surfaces are optically measured. The conditions of the simulation and the experiments are independently adjusted to match. Agreement and diversity shows upon the usefulness and limitation of wear modeling of this type.

1. Introduction

The prediction of wear and scuffing risk in metallic contacts is an important task. Influential factors such as temperature, elastic-plastic deformations, wear, surface topography, material properties and chemistry all contribute to the complex contact conditions.

Because of the complexity of the system, an experimental approach is often chosen. While an experimental approach is necessary, the underlying mechanisms behind the wear can prove difficult to probe by just analyzing wear scars and no information can be obtained in situ. Therefore, numerical predictions and matching against simulations is good complement to find out more about governing factors causing wear.

Early models for determination of wear, utilizing the Archard wear equation, used the initial pressure distribution throughout the wear life. This was found to give results that diverted from reality [1].

Numerical methods to study wear has been used by Podra and Andersson [2], incorporating a simple and numerically efficient contact mechanics model known as the Winkler surface model. Using this model, Flodin and Andersson [3] simulated wear of helical gears. Another example of using the same model is by Spiegelberg and Andersson [4] simulating wear in the valve bridge/rocker arm pad of a cam. As the model works well numerically, its simplicity carries the drawback that neighboring surface patches deflect independent of each other. This is only true for very special materials, under limited constraints.

More sophisticated mechanical contact models involving the interaction between contact points on each surface is used here by implementation of the DC-FFT method described Liu et al [5]. The plastic deformation is included by the methods of Sahlin et al. [6, 7]. This deformation behavior correspond to an ideal plastic behavior of ductile materials, such as steel.

In this study influence of elastic perfectly plastic deformations and wear is simulated for two surfaces. Under consideration of the surface asperities mutual influence by FFT-accelerated numerical methods, deeper insight into the wear mechanism of a tribosystem is expected. Numerical simulations of a sphere on a flat are compared to experimental assessments of the reciprocating motion of a ball on a disk.

Email addresses: joel.andersson@ltu.se (J. Andersson), andreas.almqvist@ltu.se (A. Almqvist), roland.larsson@ltu.se (R. Larsson)

April 29, 2010

2. Wear model

Holm [8] introduced the concept of wear volume per sliding distance, Q, being proportional to the normal force for each material pair according to

$$Q = K\frac{F}{H}. \quad (1)$$

Where H is the hardness. The wear constant K was interpreted as number of abraded atoms per atomic collision. Archard [9] improved the theory behind Eq. (1) which is known as the "Archard wear equation". The wear constant was instead interpreted as the probability that an asperity collision would lead to the formation of a wear particle. The model has been used to predict wear in several different systems, thus being used as a rough universal wear volume predictor. In this work the Archard wear equation will be interpreted as contribution to wear from tangential stresses and sliding at the micro scale. Of particular interest is wear depth at each point on the surface, h. Rewriting Eq. (1) results in

$$h = kps. \quad (2)$$

Here, the dimensional Archard wear coefficient $k = K/H$ is used as the proportionality constant to the pressure p times the sliding distance s. A localized discrete version of Eq. (2) is used. This will mean that the wear rate is constant during the sliding. by assuming lateral wear to occur at a point subjected to the pressure p over a sliding distance Δs at a magnitude of Δh.

$$\Delta h = kp \cdot \Delta s. \quad (3)$$

3. Numerical model

The numerical model has been set up to reflect the experiments that will be described under experimental details.

3.1. Contact mechanics

As real materials experience plastic flow at high pressure, plastic deformation is included in this simulation. To maintain necessary numerical efficiency the transition to fully plastic flow is immediate above yield pressure. Yield pressure is set to the same magnitude as the hardness, H. Elastic deflection due to contact between two surfaces has been solved by a fast DC-FFT method [5]. The methods of [6] and [7] are implemented for the perfectly plastic flow.

For numerical simulations the surfaces are assumed to be isotropic infinite half-spaces. The top surface is a half space shaped like a sphere with a radius of 5 mm and the opposing surface is a perfectly flat half-space. Both surfaces have elastic moduli of 207 GPa, Poisson ratios of 0.3 and a hardness of 4 GPa. The simulated load is 100 N.

3.2. Wear modelling

As the simulations are to be compared to an experiment described under experimental details, a specification of the movement is necessary. Here a wear model is used to represent the movement. Time and velocity is simulated by discrete time increments of $\Delta T = 0.25$ s at a fictional velocity $v = 0.1$ m/s. A wear constant is chosen resulting in the same wear volume as in the experiments, $k = 3.11 \cdot 10^{-16}$ Pa^{-1}.

Since the pressure on any contact point on the disk in the experiment changes with time relative to any coordinate system in the bulk of the disk, the material removal is distributed over the flat. This distribution of the wear is what will represent the relative movement of the surfaces. To achieve the distribution, a sliding direction is chosen. Along this sliding direction the wear must follow Eq. (3), considering that the pressure is different in each contact point. Figure 1 illustrates how a pressure distribution across the contact is smeared out in the sliding direction.

The pressure in each individual point on the flat will change as the sphere moves across the flat. The points close to the centre of the track on the flat would be expected to initially experience pressure for a longer time at each passing, and also experience a different pressure distribution due to the shape of the sphere. If the pressure is assumed constant during the time step ΔT and the frequency f(here $f = 25$) of the movement at constant velocity is chosen as an integer value of the time step, every worn point in the

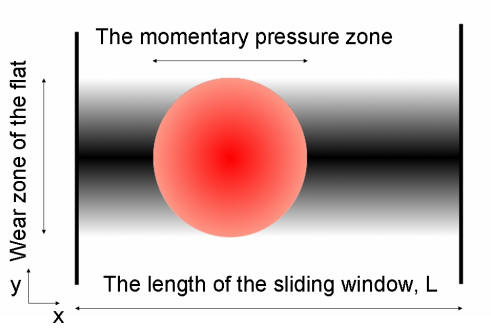

Figure 1: In order to simulate wear across the flat surface, the momentary pressure is spread out over the wear region before it is used to calculate wear in Eq. (3), giving a time avarage wear. The red shaded zone represents a possible pressure distribution at one time step. The corresponding wear on the flat would be distributed across the shaded black area, in this case resulting in more wear at the centre of the wear zone.

y-direction on the flat can be assumed to experience the whole pressure spectrum. Therefore, the time avarage pressure is equal to the geometrically avarage pressure over the whole contact region.

Shortly, the pressure average over one time step $P_p(y)$ in each contact point on the flat, choosing the sliding direction as x in Fig. 1 is determined by

$$P_p(y) = \frac{1}{N}\int_0^L P(x,y)\partial x. \qquad (4)$$

Here, L represents the length of the entire window of the flat which is worn. In the current case this window is set to 2 mm. The resulting wear height $\Delta h(y)$ on the flat over the timestep Δt is given by combining Eq. (3) with Eq. (4), that is

$$\Delta h(y) = k \cdot \frac{1}{N}\int_0^L P(x,y)\partial x \cdot \Delta t \cdot v. \qquad (5)$$

Equation (5) is implemented at each timestep with the a pressure distribution.

For the spherical surface the local pressures are used directly to calculate wear according to Eq. (3) with the same s and k. The wear is distributed equally between the surfaces.

The resulting numerically convenient model describes an ideal process of wear and deformation for a sphere moving on a flat. The model corresponds to the conditions in the middle of the disk, so the simulation should be compared to the centre of the wear scar on the disk.

4. Experimental details

Before and after experiments the contacting surfaces were measured with an optical profilometer, WYKO NT1100, manufactured by Phoenix Arisona USA. Measurements were taken at three different magnifications, rendering samples of size 1.24mm × 0.94mm, 0.62mm × 0.47mm and 0.31mm × 0.24mm. This was achieved using a 10× mirau objective with three variations of the field of view lens; producing measurements at 5×, 10× and 20× magnification.

The experiments are conducted with a sliding reciprocating rig, Optimol SRV reciprocating friction and wear tester. The rig is used to estimate surface behavior at reciprocating wear, see e.g. Hardell et al. [10].

A ball sliding on a disk, both of AISI25100 steel are the samples used in the reciprocating wear tester. The contact is lubricated with 99% pure hexadecane. The hexadecane has low polarity and should minimize chemical interaction (see e.g. Kajdas et al. [11, 12, 13] or Naveira-Suarez et al. [14]) with the surface and still reduce the friction to boundary lubrication levels. The radius of the ball is 5mm. The temperature is preset to 90°C before the samples are loaded with 100 N and the ball is slid on the disk by a frequency of 25 Hz. A stroke length of 2 mm giving an average velocity of 0.1 m/s is chosen. The test is terminated after 1 hour of sliding.

Before and after the experiment the contacting bodies were weighed in order to measure the wear-volume.

5. Results and discussion

5.1. Experimental

The weight of the disk before and after the experiment was measured to 27.6445 g and 27.6443 g respectively, i.e. a weight change of around 0.2 mg. The corresponding change of the balls weight was around 2 mg. This indicates a difference between fundamental assumptions of the numerical

model and the experiment, implying that the wear is 10 times greater on the ball than on the disk. The resulting dimensional Archard wear coefficient, using the density of the steel 7850 kg/m^3, is calculated to $K = 3.11 \cdot 10^{-16}$ Pa^{-1}.

Surface metrology measurements of the disk surface with the interferometer resulted in R_a values ranging from $6.7 - 10.8$ nm, calculated by Veeco's software Vision 32. The variations due to magnification were small, which indicates no unwanted curvature on the disk surface. The fact that we have variation in R_a value is the normal dependence on spot, resolution, measured area and measurement quality.

A surface roughness measurement of the disk is displayed in Fig. 2. Figure 3 shows the ball surface before the test. After running the test for

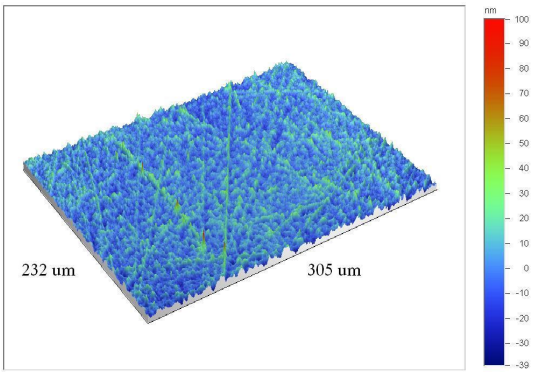

Figure 2: The roughness of the disk surface before wear.

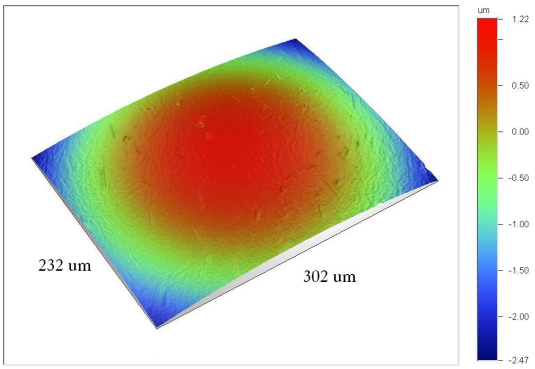

Figure 3: The ball surface before wear.

one hour, under the severe wear conditions described under experimental details, the surfaces were once again analyzed by the optical profiler system. The worn ball can be seen in Fig. 4 and

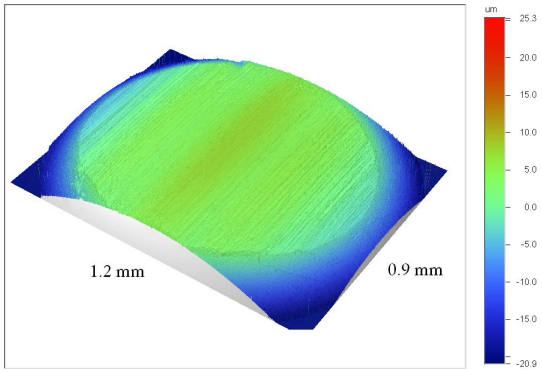

Figure 4: The wear scar on the ball.

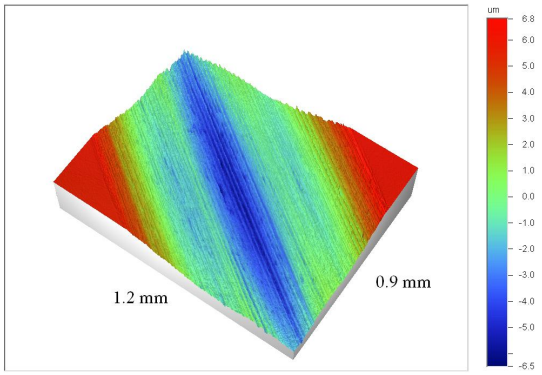

Figure 5: The wear scar on the disk.

the wear scar on the disc is depicted in Fig. 5. Severe plastic flow combined with wear has produced chaotic roughness levels. Except for the roughness there are some interesting phenomena or specific patterns, that can be seen in the wear scar, which demand an explanation.

Comparing the surface profile parallel with and perpendicular to the wear scar clearly illustrates such a pattern. Figures 6 and 7 shows worn profiles of the ball in the perpendicular and parallel directions to sliding direction respectively. From Fig. 6 it can be seen that the shape of the ball has been worn down to be almost flat, the variation in height between the end of the wear scar and the highest roughness peaks being about 1 μm. The profile seen in Fig. 7 has retained a more circular shape, with a corresponding difference in wear scar depth of about 10 μm. Two grooves has formed on each side of the centre of the wear scar. The corresponding roughness on the flat conforms as far as the wear scar is concerned, compare Fig. 5.

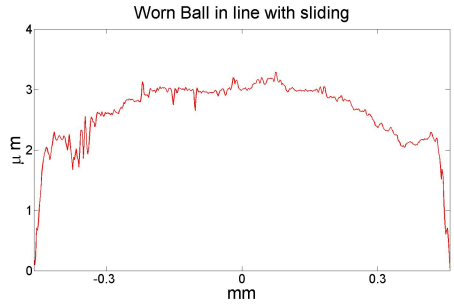

Figure 6: A typical profile of the ball parallel to the wear scar.

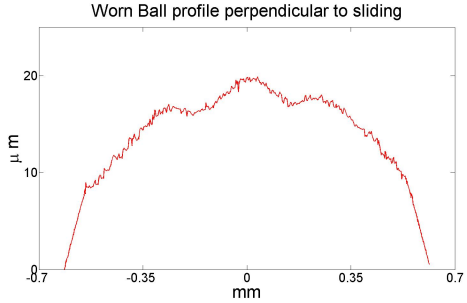

Figure 7: A typical profile of the ball perpendicular to the wear scar.

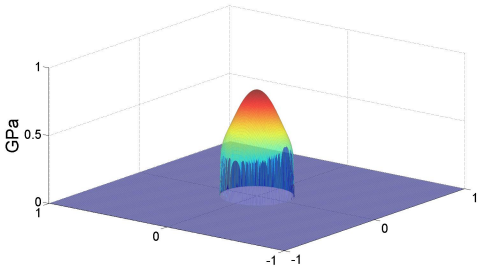

Figure 8: The complete pressure in the contact between the sphere and flat after 200 s.

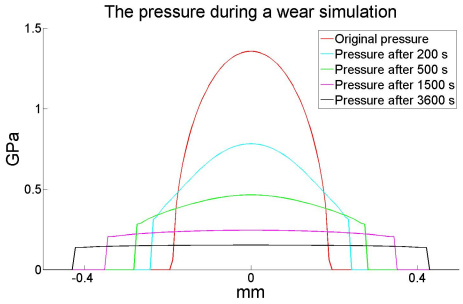

Figure 9: The pressure as it changes over time during the simulation.

If intrinsic properties of the system considered in the numerical simulations bring about the wear in the experiments, we should find identifiable similarities. In other words, how well does the Archard wear equation applied as in the numerical model describe the wear mechanism.

5.2. Numerical

The simulation of the contact between the sphere moving on the flat is described in the section numerical model. Analysis of the simulated worn profiles show both interesting similarities and differences compared to the experiment.

The contact pressure during sliding can not easily be followed in an experiment. This real time pressure is one of the advantages of using a numerical model compared to experiments. An image of the full in-contact pressure distribution after 200 s is shown in Fig. 8. Curves illustrating a cross section of the initial pressure, and the pressure after 200 s, 500 s, 1500 s and 3600 s are depicted in Fig. 9.

As can be seen the load is spread out over a larger area as the surfaces wear, leading to a lower more even pressure distribution with time. We can also see that the magnitude of the pressure is not high enough to cause plastic flow. For improvement of the model, the local pressures due to roughness should be investigated since they are likely to induce plastic flow.

Figures 10 and 11 show the wear profiles perpendicular and parallel to the sliding direction. It can be seen, by comparing to the experimental profiles, that the numerical wear model produces a profile somewhat different from that observed in the experiment on the ball. No sings of the two grooves perpendiuclar to sliding direction are seen. The basic shape of the wear scar, on the other hand, is similar in experiment and simulation. The similarity lies within the flatness seen in profiles in line with sliding, compared to the curved shape that appears perpendicular to the sliding direction. In the experiment this difference is clear comparing the y-scale in Fig. 7 and Fig. 6. It seems like the pressure distribution and the sliding distance are factors influencing wear and that the Archard model can be used to give an idea of were there is risk for wear locally.

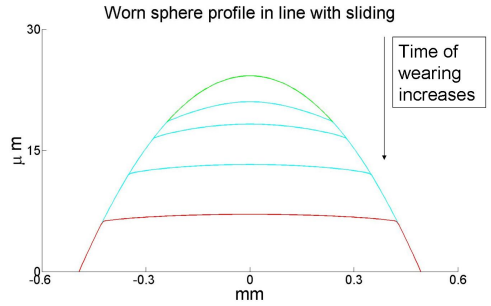

Figure 10: Profiles of a sphere being worn by a numerical model in line with the simulated sliding direction. The top curve shows the unworn surface, with profiles after 200 s, 500 s, 1500 s and finally 3600 s of wear following beneath it.

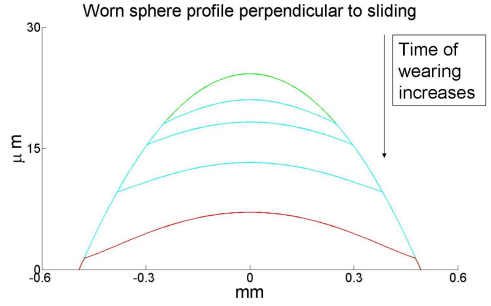

Figure 11: Profiles of a sphere worn being worn by a numerical model perpendicular to the simulated sliding direction. The top curve shows the unworn surface, with profiles after 200 s, 500 s, 1500 s and finally 3600 s of wear following beneath it.

6. Conclusions

Experimental results from a ball and disk rig have been compared to a simulation of the contact mechanics of a spherical and a flat surface. A roughness increase, i.e. an increase in R_a, was observed in the surface metrology measurement of the real worn surfaces. The wear process was also analyzed by an evaluation of the artificially worn surfaces resulting from the numerical simulations.

A direct conclusion from the experiment from the quantitative wear 10 times larger on the ball compared to the disk. It could be explained by a wear temperature dependence, since the ball is constantly in contact and will experience more friction heating and less time for recovery compared to the local parts of the disk in contact.

Simulations with the Archard wear equation was found to match to some degree with the wear on a ball and a flat. The difference on the wear scar on a ball between sliding direction and perpendicular direction was found to be intrinsic properties of the system, i.e. the pressure calculated by contact mechanical methods has been shown to have an effect on the wear. Indeed, simulations may serve as a feasible analytical tool to understand, predict and prevent wear. Still, wear modelling of this type is in an infant stage and additional effects must be added. Some examples of such effects are those from temperature and lubrcant-surface interaction.

References

[1] W.G. Sawyer. Wear predictions for a simple-cam including the coupled evolution of wear and load. *Lubrication Engineering*, 57(9):31–36, 2001.

[2] P. Podra and S. Andersson. Wear simulation with the winkler surface model. *Wear*, 207(1-2):79–85, 1997.

[3] A. Flodin and S. Andersson. A simplified model for wear prediction in helical gears. *Wear*, 249(3-4):285–292, 2001.

[4] C. Spiegelberg and S. Andersson. Simulation of friction and wear in the contact between the valve bridge and rocker arm pad in a cam mechanism. *Wear*, 261(1):58–67, 2006.

[5] S. Liu, Q. Wang, and G. Liu. A versatile method of discrete convolution and fft (dc-fft) for contact analyses. *Wear*, 243(1-2):101–111, 2000.

[6] F. Sahlin, R. Larsson, Andreas Almqvist, P.M. Lugt, and P. Marklund. A mixed lubrication model incorporating measured surface topography. part 1: theory of flow factors. *Proceedings of the Institution of Mehcnical Engineers Part J: Journal of Engineering Tribology*, 224(4):335–351, 2010.

[7] F. Sahlin, R. Larsson, Andreas Almqvist, P.M. Lugt, and P. Marklund. A mixed lubrication model incorporating measured surface topography. part 2: roughness treatment, model validation, and simulation. *Proceedings of the Institution of Mehcnical Engineers Part J: Journal of Engineering Tribology*, 224(4):353–365, 2010.

[8] R. Holm. *Electric contacts handbook*. Springer, 1958.

[9] L. Archard, J. Contact and rubbing of flat surface. *Journal of applied physics*, 24:981988, 1953.

[10] J. Hardell and B. Prakash. Tribological performance of surface engineered tool steel at elevated temperatures. *International Journal of Refractory Metals and Hard Materials*, 28(1):106–114, 2010.

[11] C. Kajdas, M. Makowska, and M. Gradkowski. Influence of temperature on the tribochemical reactions of hexadecane. *Lubrication Science*, 15(4):329–340, 2003.

[12] M. Makowska, C. Kajdas, and M. Gradkowski. Mechanism of boundary film formation from n-hexadecane. *Lubrication Science*, 16(2):101–110, 2004.

[13] C. Kajdas, M. Makowska, and M. Gradkowski. Tribochemistry of n-hexadecane in different material systems. *Lubrication Science*, 18(4):255–263, 2006.

[14] A. Naveira-Suarez, M. Grahn, R. Pasaribu, and R. Larsson. The influence of base oil polarity on the tribological performance of zinc dialkyl dithiophosphate additives. In *2nd International Conference in Advanced Tribology, Singapore*, 2008.

Appendix A. Nomenclature

The meaning of letters used to describe variables are sumarized here.

Q = Wear volume per sliding distance[m^3/m]
K = Dimensionless wear constant.
H = Hardness[Pa].
F_N = Normal force[N].
k = Dimensional wear constant K/H[Pa^{-1}].
p = Pressure[Pa].
s = Sliding distance[m].
Δs = Sliding distance[m].
h = height change due to wear[m].
Δt = The size of one timestep[s].
v = Velocity[m/s].
L = The length of the evaluation window [m]